Transitional CP Violation in MSSM and Electroweak Baryogenesis

Koichi Funakubo[a,1]**, Shoichiro Otsuki**[b,2] **and Fumihiko Toyoda**[b,3]

[a]*Department of Physics, Saga University, Saga 840-8502 Japan*

[b]*Kyushu School of Engineering, Kinki University, Iizuka 820-8255 Japan*

Abstract

Electroweak baryogenesis depends on the profile of the bubble wall created in the first-order phase transition. It is pointed out that CP violation in the Higgs sector of the MSSM could become large enough to explain the baryon asymmetry. We confirm this by solving the equations of motion for the Higgs fields with the effective potential at the transition temperature. That is, we present an example such that the transitional CP violation is realized and show the possibility that the baryon asymmetry of the universe may be produced, if marginally, by the τ lepton interacting with the wall, when an explicit CP breaking in the Higgs sector, which is consistent with experimental bounds, is induced at the phase transition.

[1]e-mail: funakubo@cc.saga-u.ac.jp

[2]e-mail: otks1scp@mbox.nc.kyushu-u.ac.jp

[3]e-mail: ftoyoda@fuk.kindai.ac.jp

1   Introduction

Baryogenesis[1] at the electroweak phase transition (EWPT) is an attractive mechanism to explain the baryon asymmetry of the universe (BAU) because the mechanism depends on parameters that will be tested sooner or later on the earth. For the mechanism to be viable, however, some extension of the standard model is required to guarantee first-order EWPT and to incorporate other sources of CP breaking than the CKM phase.

Among possible extensions of the standard model, the minimal supersymmetric standard model (MSSM) may be a well-motivated one. The MSSM could cause a strongly first-order phase transition when one of the stops is light[2, 3] and has some sources of CP breaking, though they are constrained by measurements of the neutron electric dipole moment (EDM)[4, 5]. On the other hand, another source of CP violation is relative phase θ of the vacuum expectation values (VEVs) of the two Higgs doublets[6]. The Higgs VEVs including the phase, which characterize an expanding bubble wall created at the first-order EWPT, vary spatially. Such CP violation affects propagation of quarks and leptons through their Yukawa couplings and that of charginos, neutralinos and sfermions through their mass matrices, so that weak hypercharge is carried by these particles into the symmetric phase region, where the hypercharge will be turned into baryon number by sphaleron processes.

In previous papers[7, 8], we attempted to determine the profile of the bubble wall by solving equations of motion for an effective potential V_{eff} at the transition temperature T_C in the two-Higgs-doublet model under some discrete symmetry. For a phenomenological set of the effective parameters, we presented a solution such that the CP-violating phase θ spontaneously generated becomes as large as $O(1)$ around the wall, while it completely vanishes in the broken and symmetric vacua. We shall refer to this mechanism as *transitional CP violation.* This solution yields the hypercharge flux by the quark or lepton transport to generate the BAU. We also showed [9] that a possible explicit CP breaking in the Higgs sector at T_C does *nonperturbatively* resolve the degeneracy between the CP-conjugate pair of the bubbles and leave a certain amount of BAU after the EWPT. Although several necessary conditions for the transitional CP violation were found in the MSSM[10][1], we must solve the equations for the wall profile in order to confirm that such a mechanism works in practice.

In the present article, we investigate possibility of the transitional CP violation in the MSSM. First of all in §2, we study the effective potential at T_C following a method proposed by one of the authors(K. F.)[12]. It is approximated by polynomials in the Higgs fields whose coefficients are given by the effective parameters[10, 13, 14]. In particular, we also point out that an explicit CP breaking in the Higgs sector, which is induced through loop corrections from the SUSY particles, could be enhanced at the EWPT. Employing the approximated effective potential, the equations of motion for classical field configurations are derived to find a CP-violating profile of a bubble wall in §3. In §4, we give one of numerical examples of the effective parameters which, at zero temperature, produce mass spectrum consistent with present observations. The global structure of the effective potential suggests that two degenerate minima of it are connected by a path with almost constant $\tan\beta$, where $\tan\beta$ is the ratio of the expectation values of

---

[1]As for studies including nonperturbative effects by use of 3d effective theory, see [11]

the two Higgs doublets[2]. This justifies to neglect spatial dependence of $\tan \beta$ so that the number of unknown functions is reduced. Though the bubble wall is rather broad, transitionally CP-violating solutions by the effective parameters may produce the BAU by the τ lepton transport, if marginally, when the explicit CP breaking in the Higgs sector is induced from complex parameters consistent with the neutron EDM measurement. A summary and discussions are given in §5. Formulae for the effective parameters are given in Appendix A.

2 Effective Potential and Transitional CP Violation

Let us parameterize the Higgs doublets of the MSSM as

$$\varphi_d = \frac{1}{\sqrt{2}} \begin{pmatrix} \rho_1 \\ 0 \end{pmatrix} = \frac{1}{\sqrt{2}} \begin{pmatrix} v_1 \\ 0 \end{pmatrix}, \varphi_u = \frac{1}{\sqrt{2}} \begin{pmatrix} 0 \\ \rho_2 \mathrm{e}^{i\theta} \end{pmatrix} = \frac{1}{\sqrt{2}} \begin{pmatrix} 0 \\ v_2 + iv_3 \end{pmatrix}, \qquad (2.1)$$

where $\theta \equiv \theta_1 - \theta_2$. The most general potential for them at the tree level, which is gauge invariant and renormalizable, is given as

$$
\begin{aligned}
V_0 &= m_1^2 \varphi_d^\dagger \varphi_d + m_2^2 \varphi_u^\dagger \varphi_u + (m_3^2 \varphi_u \varphi_d + \mathrm{h.c}) \\
&\quad + \frac{\lambda_1}{2} (\varphi_d^\dagger \varphi_d)^2 + \frac{\lambda_2}{2} (\varphi_u^\dagger \varphi_u)^2 + \lambda_3 (\varphi_u^\dagger \varphi_u)(\varphi_d^\dagger \varphi_d) + \lambda_4 (\varphi_u \varphi_d)(\varphi_u \varphi_d)^* \\
&\quad + \left[\frac{\lambda_5}{2} (\varphi_u \varphi_d)^2 + (\lambda_6 \varphi_d^\dagger \varphi_d + \lambda_7 \varphi_u^\dagger \varphi_u) \varphi_u \varphi_d + \mathrm{h.c} \right].
\end{aligned}
\qquad (2.2)
$$

Here the coefficients are as follows:

$$
\begin{aligned}
m_1^2 &= \tilde{m}_d^2 + |\mu|^2, \qquad m_2^2 = \tilde{m}_u^2 + |\mu|^2, \qquad m_3^2 = \mu B, \\
\lambda_1 &= \lambda_2 = \frac{1}{4}(g_2^2 + g_1^2), \qquad \lambda_3 = \frac{1}{4}(g_2^2 - g_1^2), \qquad \lambda_4 = -\frac{1}{2}g_2^2, \qquad (2.3) \\
\lambda_5 &= \lambda_6 = \lambda_7 = 0, \qquad (2.4)
\end{aligned}
$$

where $g_{2(1)}$ is the $SU(2)(U(1))$ gauge coupling and μ is the coefficient of the Higgs quadratic interaction in the superpotential. The mass squared parameters $\tilde{m}_u^2$, $\tilde{m}_d^2$ and μB come from the soft SUSY-breaking terms so that they are arbitrary at this level. m_3^2 could be complex but its phase can be eliminated by rephasing the fields when $\lambda_5 = \lambda_6 = \lambda_7 = 0$. We adopt the convention in which this m_3^2 is real and positive.

2.1 Effective potential

The effective potential up to the one-loop terms of radiative and finite-temperature corrections is

$$V_{\mathrm{eff}} = V_0 + V_1(\rho_i, 0) + V_1(\rho_i, T), \qquad (2.5)$$

where

$$V_1(\rho_i, 0) = \sum_j \frac{n_j}{64\pi^2} m_j^4 \left[\log \left(\frac{m_j^2}{M_{\mathrm{ren}}^2} \right) - \frac{3}{2} \right], \qquad (2.6)$$

---

[2]It is also reported that the spatial dependence of β is very small: $\Delta\beta \simeq O(10^{-3})$[15].

$$V_1(\rho_i, T) = \frac{T^4}{2\pi^2} \sum_j n_j J_\pm \left(a_j^2 = \frac{m_j^2}{T^2} \right), \tag{2.7}$$

with

$$J_\pm(a_j^2) = \int_0^\infty dx\, x^2 \log \left(1 \pm \exp[-\sqrt{x^2 + a_j^2}] \right). \tag{2.8}$$

Here we consider the contributions of gauge bosons, top quark, top squarks ($\tilde{t}$), charginos($\chi^\pm$) and neutralinos (χ^0). The n_i counts the degrees of freedom of each species including its statistics, that is, $n_j > 0 (n_j < 0)$ for bosons (fermions). The m_j, which is a function of the Higgs background (ρ_i, θ), is the mass of the particle. The mass matrices of the charginos, neutralinos and stops are given in Appendix[3].

We assume $M_1 = M_2$ for the gaugino mass parameters in the mass matrices, which simplifies the neutralino contributions so as to be proportional to the chargino contributions. The coefficients in V_0 are replaced by the corresponding effective parameters in $V_{\rm eff}$. Such effective parameters that are relevant to CP violation in the Higgs sector are defined by

$$\bar{m}_3^2 = -\left. \frac{\partial^2 V_{\rm eff}}{\partial v_1 \partial v_2} \right|_0 = m_3^2 + \Delta_\chi m_3^2 + \Delta_{\tilde{t}} m_3^2, \tag{2.9}$$

$$\bar{\lambda}_5 = \frac{1}{2} \left(\left. \frac{\partial^4 V_{\rm eff}}{\partial v_1^2 \partial v_2^2} \right|_0 - \left. \frac{\partial^4 V_{\rm eff}}{\partial v_1^2 \partial v_3^2} \right|_0 \right) = \Delta_\chi \lambda_5 + \Delta_{\tilde{t}} \lambda_5, \tag{2.10}$$

$$\bar{\lambda}_6 = -\frac{1}{3} \left. \frac{\partial^4 V_{\rm eff}}{\partial v_1^3 \partial v_2} \right|_0 = \Delta_\chi \lambda_6 + \Delta_{\tilde{t}} \lambda_6, \tag{2.11}$$

$$\bar{\lambda}_7 = -\frac{1}{3} \left. \frac{\partial^4 V_{\rm eff}}{\partial v_1 \partial v_2^3} \right|_0 = \Delta_\chi \lambda_7 + \Delta_{\tilde{t}} \lambda_7, \tag{2.12}$$

where Δ_χ ($\Delta_{\tilde{t}}$) implies the one-loop corrections from charginos and neutralinos (stops) given in Appendix. Except for the light stop ($\tilde{t}_1$) contributions, Taylor expansion of the finite-temperature integrals around $\rho_i = 0$ is valid. As for the light stop, we employ the high-temperature expansion[16] to obtain

$$J_-(a_{\tilde{t}_1}^2) = -\frac{\pi^4}{45} + \frac{\pi^2}{12} a_{\tilde{t}_1}^2 (\rho) - \frac{\pi}{6} a_{\tilde{t}_1}^3 (\rho) + \lambda_- a_{\tilde{t}_1}^4 (\rho) + \dots. \tag{2.13}$$

where $a_{\tilde{t}_1}^2 (\rho) = m_{\tilde{t}_1}^2 (\rho) / T^2$ and $\lambda_- = 0.1764974$.

Finally, the effective potential up to the ρ^4-terms is expressed as

$$\begin{aligned} V_{\rm eff}(\rho_i, \theta_i) = & \frac{1}{2} \bar{m}_1^2 \rho_1^2 + \frac{1}{2} \bar{m}_2^2 \rho_2^2 - \bar{m}_3^2 \rho_1 \rho_2 \cos\theta + \frac{\bar{\lambda}_1}{8} \rho_1^4 + \frac{\bar{\lambda}_2}{8} \rho_2^4 \\ & + \frac{\bar{\lambda}_3 + \bar{\lambda}_4}{4} \rho_1^2 \rho_2^2 + \frac{\bar{\lambda}_5}{4} \rho_1^2 \rho_2^2 \cos 2\theta - \frac{1}{2}(\bar{\lambda}_6 \rho_1^2 + \bar{\lambda}_7 \rho_2^2)\rho_1 \rho_2 \cos\theta \\ & - [A\rho_1^3 + \rho_1^2 \rho_2 (B_0 + B_1 \cos\theta + B_2 \cos 2\theta) \\ & \quad + \rho_1 \rho_2^2 (C_0 + C_1 \cos\theta + C_2 \cos 2\theta) + D\rho_2^3], \end{aligned} \tag{2.14}$$

---

[3]We have used the $\overline{\rm DR}$-scheme to renormalize $V_{\rm eff}$.

where $\bar{m}_i$ and $\bar{\lambda}_i$ are the effective parameters, some of which are given above. The θ-dependent ρ^3-terms come from the light stop contributions by the high-temperature expansion[10], while the weak gauge bosons contribute to θ-independent ρ^3-terms. Note also that non-zero values of $\bar{\lambda}_5$, $\bar{\lambda}_6$ and $\bar{\lambda}_7$ are induced.

To calculate the effective potential, we give $v_0 = 246\text{GeV}$ and $\tan\beta_0$ at zero temperature as an input. Once m_3^2 at the tree level is given, the other mass parameters in the tree-level potential is fixed by minimizing the effective potential at $T = 0$[12]. At the same time, the mass of the lighter (heavier) CP-even Higgs scalar m_h (m_H) and that of the pseudoscalar m_A are evaluated from the second derivatives of the effective potential at the minimum. When the EWPT is of first order, the transition temperature T_C is determined as temperature at which $(\rho_1, \rho_2) = (0, 0)$ and $(\rho_1, \rho_2) = (v\cos\beta, v\sin\beta)$ become degenerate minima of the effective potential, where the symmetry-breaking minimum is searched for by a numerical method explained in [12]. This can easily be extended to the case with CP violation, in which θ acquires nonzero value and the Higgs scalars and pseudoscalar mix to produce new mass eigenstates[12, 17].

2.2 Spontaneous CP violation

For simplicity, we assume that all the parameters of V_{eff} are real, that is, no explicit CP breaking. Then at zero temperature CP symmetry can be spontaneously violated but the lightest scalar becomes too light to satisfy experimental lower bound[18].

Now we argue that if the EWPT is of first order, CP can be violated for broader range of acceptable parameters than at $T = 0$. Note that

$$V_{\text{eff}}(\rho_i, \theta_i) = F(\rho_1, \rho_2)\left[\cos\theta - G(\rho_1, \rho_2)\right]^2 + \theta\text{-independent terms}, \qquad (2.15)$$

where

$$F(\rho_1, \rho_2) \equiv \frac{\bar{\lambda}_5}{2}\rho_1^2\rho_2^2 - 2(B_2\rho_1^2\rho_2 + C_2\rho_1\rho_2^2), \qquad (2.16)$$

$$G(\rho_1, \rho_2) \equiv \frac{2\bar{m}_3^2 + \bar{\lambda}_6\rho_1^2 + \bar{\lambda}_7\rho_2^2 + 2(B_1\rho_1 + C_1\rho_2)}{2\bar{\lambda}_5\rho_1\rho_2 - 8(B_2\rho_1 + C_2\rho_2)}. \qquad (2.17)$$

Recall that spontaneous CP violation occurs at $T = 0$ ($B_i = C_i = 0$), only if

$$F(\rho_1, \rho_2) > 0 \qquad \text{and} \qquad -1 < G(\rho_1, \rho_2) < 1, \qquad (2.18)$$

for $(\rho_1, \rho_2) = (v_0\cos\beta_0, v_0\sin\beta_0)$. These conditions strictly restrict the range of m_3^2 so that a very light scalar inevitably results, since $\bar{m}_3^2$ must be the same order as $\bar{\lambda}_6\rho_1^2 + \bar{\lambda}_7\rho_2^2$. At the first-order EWPT, (ρ_1, ρ_2) varies from $(v\cos\beta, v\sin\beta)$ to $(0, 0)$ between the broken and symmetric phase regions. Then the conditions (2.18) could be satisfied for broader range of parameters, which are acceptable in contrast to the zero-temperature case, since the effective parameters receive finite-temperature corrections and (ρ_1, ρ_2) is not specified to a single point. In this case, there exists a CP-violating local minimum in the transient region and the bubble wall profile, which is represented by the classical Higgs configuration, could have nontrivial θ near such a minimum.

Even when $F(\rho_1, \rho_2) < 0$ for some (ρ_1, ρ_2), the bubble wall profile could acquire nontrivial CP phase as long as $-1 < G(\rho_1, \rho_2) < 1$ is fulfilled at that point. In this case, V_{eff} for the fixed (ρ_1, ρ_2) is convex upwards and its peak is located at $\theta \in (0, \pi)$. If $G(\rho_1, \rho_2)$ varies between positive and negative values along the wall profile, the minimum of V_{eff} for a fixed (ρ_1, ρ_2) travels between $\theta = \pi$ and $\theta = 0$ as ρ_i varies from the symmetric phase to the broken phase. Then there exists a CP-violating saddle point of V_{eff} in the transient region.

In any case, to realize $-1 < G(\rho_1, \rho_2) < 1$ at some (ρ_1, ρ_2), $|\bar{m}_3^2|$ at T_C must become much smaller than tree-level m_3^2 by large negative corrections. Since the correction from the charginos (stops) to m_3^2 is proportional to μM_2 (μA_t) as shown in Appendix, $\mu M_2 < 0$ and/or $\mu A_t < 0$ are required for transitional CP violation to occur. Once these parameters are provided, m_3^2 which leads to $-1 < G(\rho_1, \rho_2) < 1$ is restricted in a rather narrow range. Then the mass of the Higgs scalars and pseudoscalar are almost uniquely determined. Whether a transitionally CP-violating bubble wall is realized or not is determined finally by solving the equations of motion with the effective potential at T_C.

2.3   Explicit CP breaking

In the discussions before, all the parameters of V_{eff} are assumed to be real. However, an explicit CP breaking is necessary to avoid the complete cancellation in the net baryon number due to the symmetry $\theta \leftrightarrow -\theta$ between the wall profiles.

The origins of the explicit CP breaking in V_{eff} are those in the complex μ-parameter and SUSY-breaking parameters which depend on the phases, $\alpha_1 = \arg(\mu M_1) = \arg(\mu M_2)$ contributed from charginos and neutralinos and $\alpha_2 = \arg(\mu A_t^*)$ from stops, as given in Appendix. From these we have

$$\bar{m}_3^2 = m_3^2 + e^{i\alpha_1}\Delta_\chi^{(0)} m_3^2 + e^{i\alpha_2}\Delta_{\tilde{t}}^{(0)} m_3^2, \tag{2.19}$$

$$\bar{\lambda}_5 = e^{2i\alpha_1}\Delta_\chi^{(0)}\lambda_5 + e^{2i\alpha_2}\Delta_{\tilde{t}}^{(0)}\lambda_5, \tag{2.20}$$

$$\bar{\lambda}_6 = e^{i\alpha_1}\Delta_\chi^{(0)}\lambda_6 + e^{i\alpha_2}\Delta_{\tilde{t}}^{(0)}\lambda_6, \tag{2.21}$$

$$\bar{\lambda}_7 = e^{i\alpha_1}\Delta_\chi^{(0)}\lambda_7 + e^{i\alpha_2}\Delta_{\tilde{t}}^{(0)}\lambda_7, \tag{2.22}$$

where $\Delta^{(0)}$ denotes the corrections in the case when all the tree-level parameters are real.

The magnitudes of α_1 and α_2 will be bounded by experiments to be $O(< 10^{-3})$ or so[4]. These CP-breaking phases can be gathered on $\bar{m}_3^2$ by rephasing the Higgs fields when the contributions of the stops are very small compared with those of charginos and neutralinos. After rephasing, $\bar{m}_3^2$ is given in the form of

$$e^{-i\alpha_1}\bar{m}_3^2 = e^{-i\alpha_1}m_3^2 + \Delta_\chi^{(0)} m_3^2 \equiv e^{i\delta}|\bar{m}_3^2|, \tag{2.23}$$

so that the CP-breaking phase δ is given by

$$\tan\delta = -\frac{m_3^2 \sin\alpha_1}{m_3^2 \cos\alpha_1 + \Delta_\chi^{(0)} m_3^2}. \tag{2.24}$$

This suggests a very interesting possibility that, if $\left|m_3^2 + \Delta_\chi^{(0)} m_3^2\right| \ll m_3^2$, which is often the case for the transitional CP violation, then a somewhat large $|\delta|$ is induced even if $\sin\alpha_1 \simeq 0$.

Hereafter, we put the explicit CP breaking at T_C by replacing $\bar{m}_3^2 \cos\theta$ in V_{eff} (2.14) by $(1/2)(e^{i(\delta+\theta)}\bar{m}_3^2 + \text{h.c.})$, but consider the case of small $\delta \sim O(10^{-3})$.

3 CP-Violating Solutions

3.1 Equations of motion

We are now interested in classical solutions of the bubble wall. If the phase transition proceeds calmly, it will be valid to expect that the bubble wall grows keeping the profile of the critical bubble, which is determined by static equations of motion. Further, when the bubble is spherically symmetric and is sufficiently macroscopic so that it is regarded as a planar object, the system may be reduced to an effectively one-dimensional one. Regarding the bubble wall as a static planar object, the equations of motion are given by[7]

$$
\begin{aligned}
\frac{d^2\rho_i(z)}{dz^2} - \rho_i(z)\left(\frac{d\theta_i(z)}{dz}\right)^2 - \frac{\partial V_{\text{eff}}}{\partial\rho_i} &= 0, \\
\frac{d}{dz}\left(\rho_i^2(z)\frac{d\theta_i(z)}{dz}\right) - \frac{\partial V_{\text{eff}}}{\partial\theta_i} &= 0,
\end{aligned}
\tag{3.1}
$$

where z is the coordinate perpendicular to the wall. Furthermore, gauge configurations of the pure-gauge type with no dynamical freedom in 1+1-dimensions are expected to give the lowest energy of the system. Then, it is convenient to fix the gauge in such a way that the gauge fields disappear by imposing the condition

$$
\rho_1^2(z)\frac{d\theta_1(z)}{dz} + \rho_2^2(z)\frac{d\theta_2(z)}{dz} = 0.
\tag{3.2}
$$

The total energy density of the bubble wall per unit area is given by

$$
\mathcal{E} = \int_{-\infty}^{\infty} dz \left\{ \frac{1}{2}\sum_{i=1,2}\left[\left(\frac{d\rho_i}{dz}\right)^2 + \rho_i^2\left(\frac{d\theta_i}{dz}\right)^2\right] + V_{\text{eff}}(\rho_1,\rho_2,\theta) \right\}.
\tag{3.3}
$$

3.2 Kink ansatz

In accord with the first-order phase transition, we adopt an ansatz that the kink configuration connecting the vacua is a solution to the equations of motion. Using a dimensionless variable $y = (1/2)(1 - \tanh(az))$, we put $\rho(y) = (\rho_1/v)/\cos\beta = (\rho_2/v)/\sin\beta$ and $\theta(y) = \theta_1/\sin^2\beta = -\theta_2/\cos^2\beta$ under the gauge-fixing condition (3.2). Here a is taken to be the inverse wall thickness. The equations of motion to give $\rho(y)$ and $\theta(y)$ are read as

$$
\begin{aligned}
4y(1-y)\frac{d}{dy}\left(y(1-y)\frac{d\rho}{dy}\right) - 4\cos^2\beta\sin^2\beta y^2(1-y)^2\rho\left(\frac{d\theta}{dy}\right)^2 &= \frac{\partial W(\rho,\theta)}{\partial\rho}, \\
4\cos^2\beta\sin^2\beta y(1-y)\frac{d}{dy}\left(y(1-y)\rho^2\frac{d\theta}{dy}\right) &= \frac{\partial W(\rho,\theta)}{\partial\theta},
\end{aligned}
\tag{3.4}
$$

6

where $W(\rho(y), \theta(y)) \equiv V_{\text{eff}}(\rho_i, \theta)/a^2 v^2$ is dimensionless.

The parameterization of W convenient to the kink ansatz in the presence of δ is as follows:

$$
\begin{aligned}
W(\rho, \theta) &= \rho^2 \Big[2 + b(\cos(\theta_b + \delta) - \cos(\theta + \delta))\Big] \\
&+ \rho^4 \Big[2 + c(\cos\theta_b - \cos\theta) + \frac{d}{4}(\cos 2\theta_b - \cos 2\theta)\Big] \\
&- \rho^3 \Big[4 + e(\cos\theta_b - \cos\theta) + f(\cos 2\theta_b - \cos 2\theta)\Big].
\end{aligned}
\tag{3.5}
$$

Here $\theta_b \sim O(\delta)$ is the boundary value of θ in the broken vacuum given later. The parameters in $W(\rho, \theta)$ and those in $V_{\text{eff}}(\rho_i, \theta)$ are related as follows:

$$
\begin{aligned}
b &= (1/a^2)\bar{m}_3^2 \cos\beta \sin\beta, \\
c &= (v/a)^2(\bar{\lambda}_6 \cos^2\beta + \bar{\lambda}_7 \sin^2\beta)\cos\beta \sin\beta/2, \\
d &= -(v/a)^2\bar{\lambda}_5 \cos^2\beta \sin^2\beta, \\
e &= -(v/a^2)(B_1 \cos\beta + C_1 \sin\beta)\cos\beta \sin\beta, \\
f &= -(v/a^2)(B_2 \cos\beta + C_2 \sin\beta)\cos\beta \sin\beta,
\end{aligned}
\tag{3.6}
$$

together with relations from the kink ansatz:

$$
\begin{aligned}
\bar{m}_1^2 \cos^2\beta + \bar{m}_2^2 \sin^2\beta &= 2a^2(2 + b\cos(\theta_b + \delta)), \\
\bar{\lambda}_1 \cos^4\beta + \bar{\lambda}_2 \sin^4\beta &+ 2(\bar{\lambda}_3 + \bar{\lambda}_4)\cos^2\beta \sin^2\beta \\
&= (a/v)^2 8(2 + c\cos\theta_b + (d/4)\cos 2\theta_b), \\
A\cos^3\beta &+ (B_0 \cos\beta + C_0 \sin\beta)\cos\beta \sin\beta + D\sin^3\beta \\
&= (a^2/v)(4 + e\cos\theta_b + f\cos 2\theta_b).
\end{aligned}
\tag{3.7}
$$

Once the parameter set (b, c, e, d, f) is given, the stability of the two vacua and the condition $W(\rho, \theta) \geq 0$ in the region of $0 \leq \rho < \infty$ and $0 \leq \theta < 2\pi$ have to be checked. As it should be, in the case of $\delta = 0$, the kink solution $(\rho = 1 - y \equiv \rho_{kink}, \theta = 0)$ satisfies the equations of motion.

That $\partial W/\partial\theta|_{\rho=1} = 0$ gives the boundary value θ_b determined from

$$
\tan\theta_b = -\frac{b\sin\delta}{b\cos\delta + c - e + (d - 4f)\cos\theta_b},
\tag{3.8}
$$

and $\partial W/\partial\theta|_{\rho\simeq 0} = 0$ does the boundary value of the symmetric vacuum as $\theta_s = -\delta, \pi - \delta$. Needless to say, $\rho_b = 1$ and $\rho_s = 0$. At first sight, any θ_s might be allowed because of $\rho_s = 0$. But the energy density of the bubble wall diverges for the other θ_s.

In the case of $\delta = 0$, suppose that we obtain a nontrivial solution $(\rho \neq \rho_{kink}, \theta \neq 0)$ with the maximum of $\theta > 0$. Let us denote this solution as (ρ^0, θ^0). As explained before, we have the CP-conjugate partner of it, $(\rho^0, -\theta^0)$. Without loss of generality we choose $\delta \geq 0$ because of the symmetry $(\delta, \theta) \longleftrightarrow (-\delta, -\theta)$. For $\delta > 0$ small enough, we would have in general three types of solutions, the positive-θ solution (ρ^+, θ^+), the negative-θ solution (ρ^-, θ^-) and the small-θ solution (ρ^s, θ^s) such that, as $\delta \to 0$, the positive-θ solution tends to (ρ^0, θ^0), the negative-θ solution to $(\rho^0, -\theta^0)$ and the small-θ solution to

Table 1: Parameters adopted for the numerical calculation.

v_0	$\tan \beta_0$	m_3^2	μ	A_t	$M_2 = M_1$	$m_{\tilde{t}_L}$	$m_{\tilde{t}_R}$
246 GeV	6	8110 GeV^2	-500 GeV	60 GeV	500 GeV	400 GeV	0

the kink solution $(\rho_{kink}, \theta = 0)$. The small-$\theta$ solution has no CP-conjugate partner. For a larger δ, either of the positive-θ solution or the negative-θ one, which has the lower energy for a small δ, survives[9].

The energy density of the bubble wall is now expressed as follows, where that of the kink solution, $\mathcal{E}_{kink} = av^2/3$, is chosen as the standard:

$$
\begin{aligned}
\frac{\Delta\mathcal{E}}{av^2} &= \int_0^1 dy \Bigg[y(1-y) \left\{ \left(\frac{d\rho}{dy}\right)^2 + \cos^2\beta \sin^2\beta\, \rho^2 \left(\frac{d\theta}{dy}\right)^2 \right\} \\
&+ \frac{1}{2y(1-y)} W(\rho(y), \theta(y)) \Bigg] - \frac{1}{3}.
\end{aligned}
\tag{3.9}
$$

Let us denote as $\Delta\mathcal{E}^+$, $\Delta\mathcal{E}^-$ and $\Delta\mathcal{E}^s$ respectively for the positive-θ, negative-θ and small-θ solutions.

4   A Numerical Example of Transitional CP Violation

4.1   Numerical results of MSSM calculation

We give one of numerical examples at the EWPT and the effective parameters in the MSSM. The parameters adopted are listed in Table 1. As noted in §2.2, $\mu M_2 < 0$ and $\mu A_t < 0$ are favored for transitional CP violation. Once these parameters are given, the tree-level m_3^2 is tuned to satisfy the conditions for transitional CP violation. Since the magnitudes of the effective couplings at $T_C \sim 100$ GeV are always $10^{-3} - 10^{-2}$ when the mass parameters are taken to be between weak scale and a few TeV, an appropriate value of m_3^2 is about $O(10^4)$ GeV^2. Although it is reported that a small value of $\tan\beta_0$ is favored for a strong EWPT satisfying $v/T_C > 1$ with an acceptable Higgs mass[19], we take $\tan\beta_0 = 6$. One of reasons why we take $\tan\beta_0 = 6$ is that for the other parameters listed in Table 1, a larger $\tan\beta_0$ yields a heavier Higgs scalar when one includes contributions from charginos and neutralinos, which were often ignored in literatures[12]. Another reason is that for a large $\tan\beta_0$, it is rather easy to find a stable nontrivial wall profile, since the second kinetic term in (3.9) $\sim \cos^2\beta$ while $W(\rho, \theta) \sim \cos\beta$ as in (3.6), so that $\Delta\mathcal{E} < 0$ is realized.

The particle spectrum from this set of the parameters are given in Table 2. The transition temperature T_C and the VEVs at T_C are given by

$$
T_C = 93.4 \text{ GeV}, \quad v = 129.17 \text{ GeV}, \quad \tan\beta = 7.292,
\tag{4.1}
$$

so that $v/T_C \simeq 1.38$, which guarantees that the BAU created at the EWPT is not washed out after the transition. The values of the effective parameters near T_C are presented in

Table 2: Masses of the lighter Higgs scalar (m_h), the Higgs pseudoscalar (m_A), the heavier Higgs scalar (m_H), the lighter top squark ($m_{\tilde{t}_1}$), the lighter chargino ($m_{\chi_1^\pm}$) and the lightest neutralino ($m_{\chi_1^0}$).

m_h	m_A	m_H	$m_{\tilde{t}_1}$	$m_{\chi_1^\pm}$	$m_{\chi_1^0}$
82.28 GeV	117.9 GeV	124.0 GeV	167.8 GeV	457.6 GeV	449.8 GeV

Table 3: The effective parameters near the transition temperature $T_C = 93.4$ GeV.

T(GeV)	$(\bar{m}_3^2)_{\text{eff}}$ (GeV^2)	λ_5	λ_6	λ_7
93.3	-402.375	4.98562×10^{-3}	-1.09172×10^{-2}	7.65974×10^{-3}
93.4	-401.720	4.98684×10^{-3}	-1.09197×10^{-2}	7.65912×10^{-3}
93.5	-401.065	4.98806×10^{-3}	-1.09222×10^{-2}	7.65850×10^{-3}
93.6	-400.410	4.98928×10^{-3}	-1.09247×10^{-2}	7.65787×10^{-3}

Table 3 and

$$\frac{B_2}{T_C} = 1.5741 \times 10^{-3}, \quad \frac{C_1}{T_C} = 3.2539 \times 10^{-2}. \tag{4.2}$$

The global structure of V_{eff} at T_C is depicted in Fig. 1. The T dependence of the effective parameters are plotted in Figs. 2 and 3.

By closely investigating the saddle point between the two degenerate minima, we find that the height of the saddle point is $V_{\text{max}} = 3.6516 \times 10^9$ GeV^4, from which the inverse wall thickness a is given by [4]

$$a = \frac{\sqrt{8V_{\text{max}}}}{v} = 13.23 \text{ GeV}. \tag{4.3}$$

4.2 Transitional CP violation and BAU

From the numerical results above, we fix the parameters at T_C=93.4 GeV as v=129.2 GeV, a=13.23 GeV, $\tan\beta$=7.29 and ($b = -0.308, c = 0.048, d = -0.009, e = -0.3, f = -0.0003$). For δ=0.001 and 0.002 respectively, a pair of solutions $(\rho^+(y), \theta^+(y))$ and $(\rho^-(y), \theta^-(y))$ with $\theta_s = \pi - \delta$ are obtained, which are shown in Fig. 4 of the w_1-w_2 plain on the contour plot of $W(w_1, w_2)$, where $w_1 \equiv \rho \cos(\theta - \theta_b)$ and $w_2 \equiv \rho \sin(\theta - \theta_b)$ [5].

Bubble formation rate The bubble formation probability of the each solution is

---

[4]The solution for $\phi'' = \frac{dV_{\text{eff}}}{d\phi}$ with $V_{\text{eff}} = \frac{\lambda}{4}\phi^2(\phi - v)^2$ is given by $\phi = \frac{v}{2}(1 + \tanh az)$ with $a^2 = \frac{\lambda}{8}v^2$. This leads to $V_{\text{max}} = V_{\text{eff}}(\phi = \frac{v}{2}) = \frac{\lambda}{64}v^4 = \frac{a^2v^2}{8}$.

[5] For $b < 0(> 0)$ it is easy to show that the exit gate toward $w_1 < 0$(left) from the basin of the symmetric vacuum at $(w_1 = 0, w_2 = 0)$ is wider (narrower) than that toward $w_1 > 0$ (right) in Fig. 4. So, $b < 0(> 0)$ favors $\theta_s = \pi - \delta(= -\delta)$. Usually we have found no convergent solutions with $\theta_s = -\delta(\pi - \delta)$ for $b < 0(> 0)$ in the relaxation method. For $b < 0$ with $\tan\beta \leq 3$, no solutions have been obtained. For the smaller values of $\tan\beta$ there is a wide parameter range to admit solutions for $b > 0$. However, the parameters of them, in particular (c, d, e), are not compatible with the MSSM calculation.
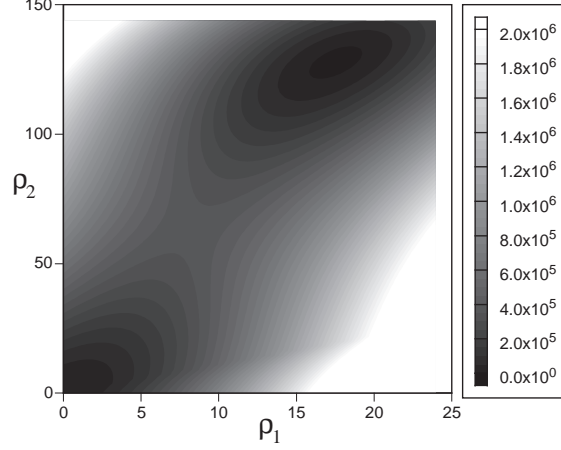
Figure 1: Contour plot of $V_{\text{eff}}(\rho_i; T_C)$ in the unit of GeV^4, where $\rho_1 = v \cos\beta$ and $\rho_2 = v \sin\beta$ in the unit of GeV.
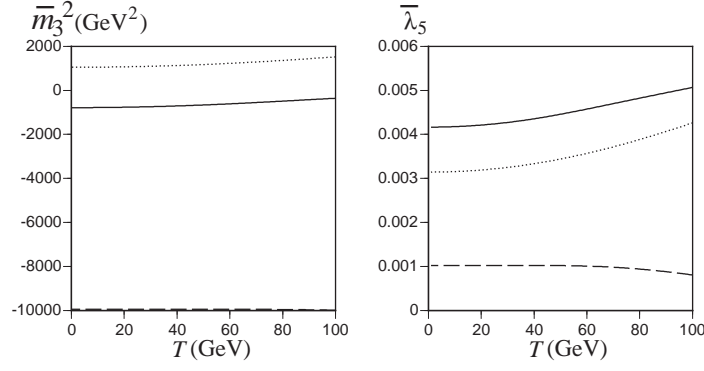

Figure 2: Behaviors of the effective parameters $(\bar{m}_3^2)_{\text{eff}}$ and $\bar{\lambda}_5$. The dashed lines represent the contributions from the charginos and neutralinos, the dotted lines represent those from the stops and the solid lines are the sum of the tree-level and one-loop contributions.
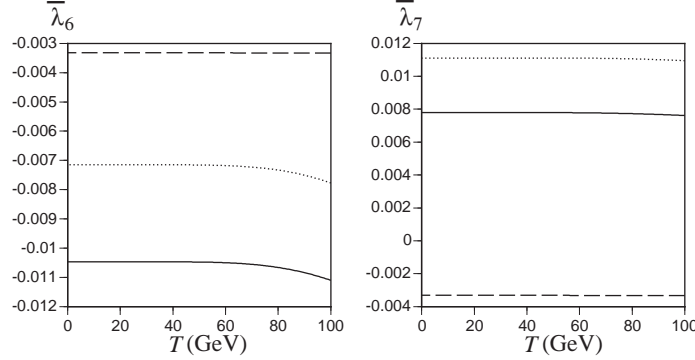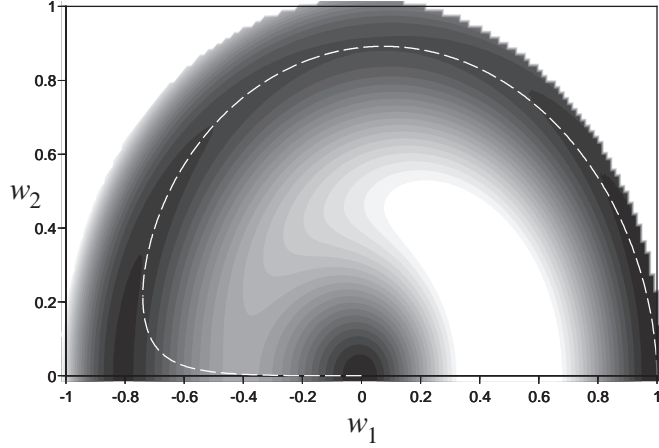

Figure 3: Behaviors of the effective parameters $\bar{\lambda}_6$ and $\bar{\lambda}_7$. The dashed lines represent the contributions from the charginos and neutralinos, the dotted lines represent those from the stops and the solid lines are the sum of the tree-level and one-loop contributions.

10

Figure 4: Contour plot of $W(w_1, w_2)$ together with the positive-θ solution for $\delta = 0.001$ (broken curve).

proportional to

$$N^\pm = \exp\left(-\frac{4\pi R_{crit}^2 \Delta \mathcal{E}^\pm}{T_C}\right), \tag{4.4}$$

where R_{crit} is the radius of the critical bubble at T_C and is given by $\sqrt{3F_{crit}/4\pi a v^2}$ and the free energy of the bubble F_{crit} is estimated as $145 T_C$. The explicit CP breaking $\delta \neq 0$, even when very small, nonperturbatively breaks the degeneracy of the CP-conjugate pair of the bubbles as mentioned before. The formation rate is

$$
\begin{aligned}
N^-/N^+ &= 0.601 \quad \text{for} \quad \delta = 0.001, \\
&= 0.361 \quad \text{for} \quad \delta = 0.002.
\end{aligned}
\tag{4.5}
$$

Chiral charge flux Once a set of solutions are given, we calculate the reflection coefficient $\Delta R(\xi, p_L/a)$ of the each solution, where p_L is the incident momentum of the particle perpendicular to the wall and $\xi = m_C/a$, m_C being the mass at T_C. That is, $m_C = m_{b(\tau)} v \cos\beta/(v_0 \cos\beta_0)$ for the bottom quark (τ lepton). Important here is that the bottom quark and the τ lepton interact with the wall magnitude $\rho(y)$ with the coupling $\sin^2\beta$ while the top quark does with $\cos^2\beta$. Therefore the top quark passes the wall almost freely for such a large $\tan\beta$ and is completely negligible for the BAU.

Then the chiral charge flux through the wall is given by[20]

$$F_Q = \frac{Q_L - Q_R}{4\pi^2\gamma} \int_{m_C}^\infty dp_L \int_0^\infty dp_T\, p_T \left[f^s - f^b\right] \Delta R(\xi, \frac{p_L}{a}), \tag{4.6}$$

where

$$f^s = \frac{p_L}{E} \frac{1}{e^{\gamma(E - u p_L)/T_C} + 1}, \qquad f^b = \frac{p_L}{E} \frac{1}{e^{\gamma(E + u\sqrt{p_L^2 - m_C^2})/T_C} + 1}, \tag{4.7}$$

are the statistical factors in the symmetric and broken phases respectively, p_T is the incident momentum of the particle parallel to the wall, $E = \sqrt{p_L^2 + p_T^2}$, u is the wall velocity and $\gamma = 1/\sqrt{1 - u^2}$.
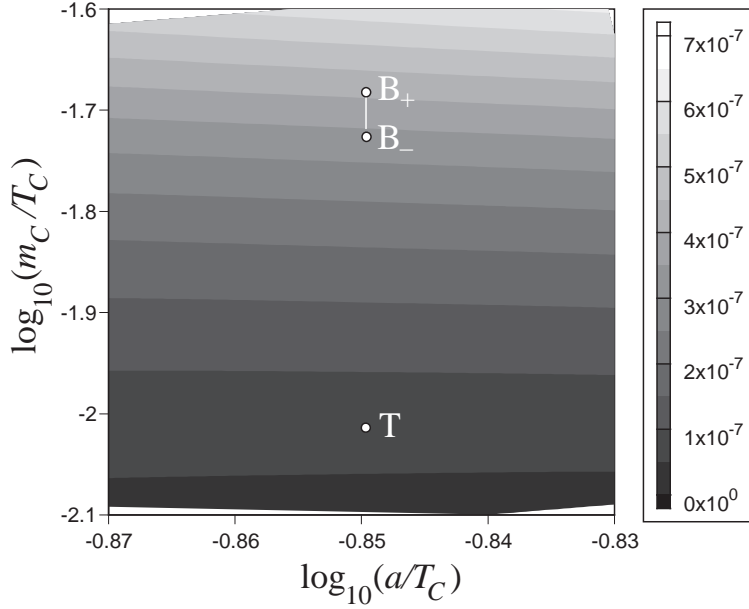
11

Figure 5: Contour plot of $F_Q^{net}/((Q^L - Q^R)T_C^3 u)$.

The net contribution to BAU is [6]

$$F_Q^{net} = \frac{N^+ F_Q^+ - N^- F_Q^-}{N^+ + N^-}. \tag{4.8}$$

Fig. 5 shows $F_Q^{net}/((Q^L - Q^R)T_C^3 u)$ for $\delta = 0.001$ and $u = 0.1$ as a contour plot on the $a/T_C - m_C/T_C$ plain. The point $B_+(B_-)$ is the b quark contribution if $m=4.4(4.1)$ GeV, and the point T is the τ lepton contribution. $F_Q^{net}/((Q^L - Q^R)T_C^3 u)$ amounts to $4 \times 10^{-7}, 3.4 \times 10^{-7}, 4 \times 10^{-8}$ at B_+, B_-, T respectively. The top of the contour hill is 6.3×10^{-3} at $\log_{10}(a/T_C) = 0.88$ and $\log_{10}(m_C/T_C) = 0.29$. As is well known, a thin wall produces a large chiral charge flux. For $\delta = 0.002$, F_Q^{net} increases as a whole by a factor of about 1.7. As u increases to 0.9, the contour at the point B_-, say, decreases by a factor of about 0.4.

From F_Q^{net} we can estimate the BAU in the transport scenario as

$$\frac{\rho_B}{s} \sim 10^{-7} \times \frac{F_Q^{net}}{u} \times \frac{\tau}{T_C^2}, \tag{4.9}$$

where the entropy density is given by $s = 2\pi^2 g_* T_C^3/45$ with $g_* \simeq 100$ and τ is the transverse time within which the scattered particles are captured by the wall. If τ is given by D/u with the diffusion constant D, it is estimated from $D(b \quad \text{quark}) \sim 1/T_C$ and $D(\tau \quad \text{lepton}) \sim (10^{2-3})/T_C$. Then

$$\begin{aligned} \rho_B/s &< 10^{-12} \quad (\text{for} \quad b \quad \text{quark}), \\ \rho_B/s &\sim 10^{-(10-12)} \quad (\text{for} \quad \tau \quad \text{lepton}) \end{aligned} \tag{4.10}$$

---

[6] For the parameter set with $b < 0$, we have found no small-θ solutions because the wider exit gate from the symmetric vacuum has the direction just opposite toward the broken one at $(w_1 = 1, w_2 = 0)$. Even in the case when the small solution exists, $\Delta \mathcal{E}^s$ is negligibly small.

for $\delta = 0.001$ and $u = 0.1$. Thus our example may give a possibility to produce the BAU by the transitional CP violation of the τ lepton, if marginally, in the MSSM, provided that $\delta \sim O(10^{-3})$ is induced.

5   Summary and Discussions

We have shown the possibility of the transitional CP violation in the MSSM. For this scenario to be realized, some of the parameters in the theory are constrained: $\mu M_2 < 0$ and/or $\mu A_t < 0$ are required, m_3^2 should be $O(10^4)\,\text{GeV}^4$, and $\tan\beta_0 \geq 5$ would be necessary for our choice of the mass parameters to have the lightest Higgs scalar with an acceptable mass and to have nontrivially CP-violating wall profile. These requirements inevitably relate the mass of the Higgs scalar to that of the pseudoscalar.

Although the explicit CP breaking in the Higgs sector is severely limited from the neutron EDM at $T = 0$, that induced at T_C can be somewhat large. If the latter is $\delta \sim O(10^{-3})$ and breaks the degeneracy between the pair of CP-conjugate bubbles, our numerical example could be able to produce the BAU$\sim O(10^{-10})$ by the τ lepton transport. The θ-dependent ρ^3-terms essential for the transitional CP violation is induced only if one of the soft SUSY-breaking masses, $m_{\tilde{t}_R}$ of the stop, almost vanishes. This implies that the mass of the lighter stop $m_{\tilde{t}_1}$ must satisfy $m_{\tilde{t}_1} \lesssim m_t$.

Our result of a rather thick walls, $1/a \sim 10/T_C$ together with a large $\Delta\theta = |\theta_b - \theta_s| \sim \pi$ may favor the diffusion scenario[21], although estimating various uncertain factors of this scenario is outside the scope of this article.

In §2.2, we have pointed out another possibility of transitional CP violation associated with $F(\rho_1, \rho_2) < 0$. A wall profile of this type, if exists, will generate sizable BAU just as the example presented here, since θ varies from 0 to π. As long as the high-temperature expansion of the light stop contributions is valid, the B_2-term in (2.16) is negligible compared to the $\bar{\lambda}_5$-term. Indeed we found a well qualified solutions for $(d = -0.009, f = -0.0003)$, which is obtained from the parameter set studied here only by changing the sign of d. It is, however, difficult to have negative $\bar{\lambda}_5$ and $|G(\rho_1, \rho_2)| < 1$ for an intermediate (ρ_1, ρ_2) with an acceptable set of parameters when $m_{\tilde{t}_R} = 0$. This can be seen as follows. As shown in [10], $\Delta_{\tilde{t}}m_3^2/(\mu A_t)$ and $\Delta_{\tilde{t}}\lambda_5/(\mu A_t)^4$ are functions of T and $m_{\tilde{t}_L}$ when $m_{\tilde{t}_R} = 0$. These are plotted for $\tan\beta_0 = 6$ at $T = 95$ GeV in Fig. 6. Contour plots of the chargino-neutralino contributions $\Delta_\chi m_3^2$ and $\Delta_\chi \lambda_5$ for $\tan\beta_0 = 6$ and $T = 95$ GeV are shown in Fig. 7. In order for $\bar{\lambda}_5$ to be negative, rather small $|\mu M_2|$ is required. Since $|\Delta_\chi \lambda_5|$ is at most $O(10^{-4})$ in the region where $\Delta_\chi \lambda_5$ is negative, $|\mu A_t|$ must be smaller than 10^4 GeV^2 to have negative $\bar{\lambda}_5$. As seen from Fig. 7, $\Delta_\chi m_3^2 > 1500$ GeV^2 in the region where $\Delta_\chi \lambda_5 < 0$. As long as we take $m_{\tilde{t}_L}$ larger than the weak scale, $\Delta_{\tilde{t}}m_3^2 \sim -0.1 \cdot \mu A_t$, so that $\Delta_{\tilde{t}}m_3^2$ should be larger than -1000 GeV^2. Hence to satisfy $|G(\rho_1, \rho_2)| < 1$, the tree-level m_3^2 must be taken to be at most 2500 GeV^2. This small m_3^2 inevitably produces too light Higgs bosons, which are inconsistent with the present bound $m_h \geq 67.5$ GeV and $m_A \geq 67.5$ GeV[22]. We have examined cases with larger $\tan\beta_0$, which yield heavier Higgs bosons, but find no region in the parameter space that both $\bar{\lambda}_5 < 0$ and $|G(\rho_1, \rho_2)| < 1$ are satisfied with acceptable Higgs masses. Although this interesting scenario of CP violation is far from realizable in the MSSM, a general two-
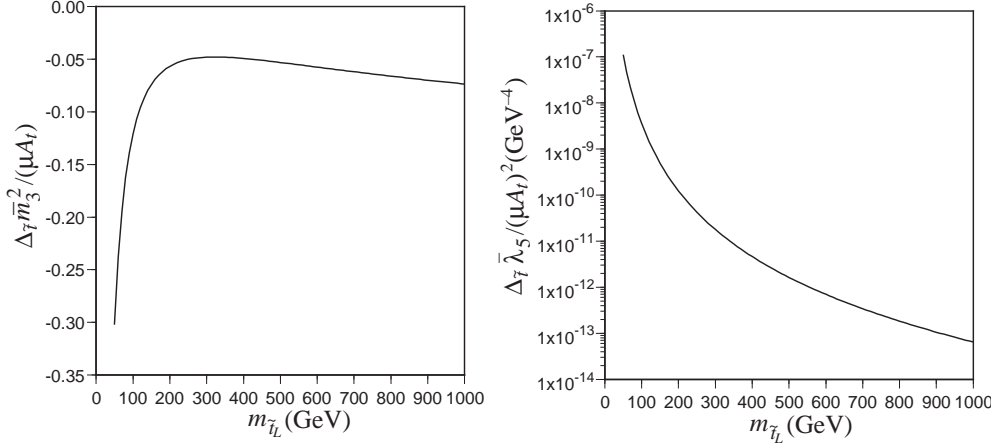
Figure 6: $\Delta_{\tilde{t}} m_3^2/(\mu A_t)$ and $\Delta_{\tilde{t}} \lambda_5/(\mu A_t)^2$ for $\tan \beta_0 = 6$ at $T = 95$ GeV.
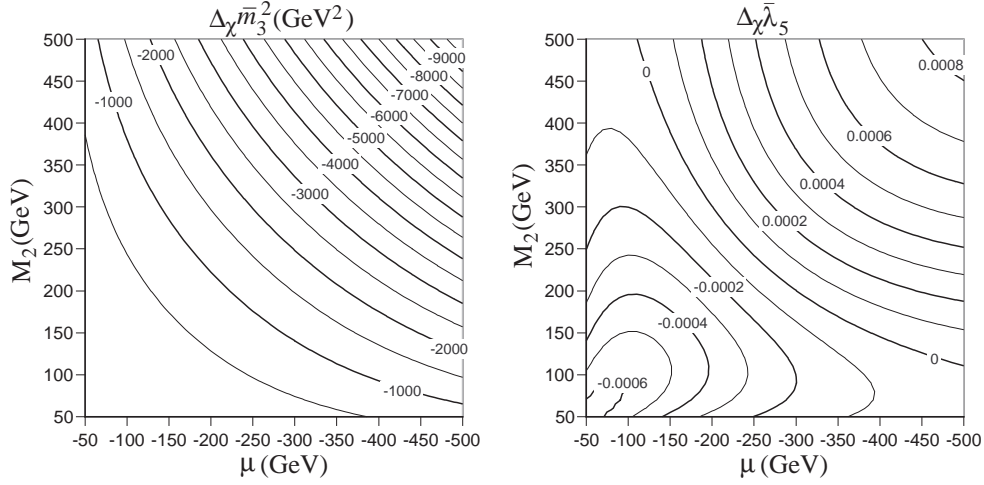

Figure 7: Contour plots of $\Delta_\chi m_3^2$ and $\Delta_\chi \lambda_5$ at $T = 95$ GeV.

Higgs-doublet model will allow a wall profile with $\bar{\lambda}_5 < 0$, since it has nonzero tree-level λ_5 as a free parameter and we confirmed the existence of such a solution.

Acknowledgment

A   Formulas for the Effective Parameters

In this appendix, we summarize the contributions from the charginos, neutralinos and stops to the effective parameters. As for the formulas to evaluate the finite-temperature Feynman integrals, refer to Appendix of [10].

The mass matrices of the charginos and neutralinos are given by

$$M_{\chi^\pm} = \begin{pmatrix} M_2 & -\frac{ig_2}{\sqrt{2}}\rho_2 e^{-i\theta} \\ -\frac{ig_2}{\sqrt{2}}\rho_2 & -\mu \end{pmatrix}, \tag{A.1}$$

$$M_{\chi^0} = \begin{pmatrix} M_2 & 0 & -\frac{i}{2}g_2\rho_1 & \frac{i}{2}g_2\rho_2 e^{-i\theta} \\ 0 & M_1 & \frac{i}{2}g_1\rho_1 & -\frac{i}{2}g_1\rho_2 e^{-i\theta} \\ -\frac{i}{2}g_2\rho_1 & \frac{i}{2}g_1\rho_1 & 0 & \mu \\ \frac{i}{2}g_2\rho_2 e^{-i\theta} & -\frac{i}{2}g_1\rho_2 e^{-i\theta} & \mu & 0 \end{pmatrix}, \tag{A.2}$$

respectively. Here M_1 and M_2 are the gaugino mass parameters. The contributions from the charginos are given by

$$\Delta_{\chi^\pm}m_3^2 = 2g_2^2\mu M_2 \cdot i \int_k \Delta_1(k)\Delta_\mu(k), \tag{A.3}$$

$$\Delta_{\chi^\pm}\lambda_5 = -2g_2^4(\mu M_2)^2 \cdot i \int_k \Delta_1^2(k)\Delta_\mu^2(k), \tag{A.4}$$

$$\Delta_{\chi^\pm}\lambda_6 = \Delta_{\chi^\pm}\lambda_7 = 2g_2^4\mu M_2 \cdot i \int_k k^2 \Delta_1^2(k)\Delta_\mu^2(k), \tag{A.5}$$

and those from the neutralinos are

$$\Delta_{\chi^0}m_3^2 = 2i \int_k \left[g_2^2\mu M_2\Delta_1(k)\Delta_\mu(k) + g_1^2\mu M_1\Delta_2(k)\Delta_\mu(k)\right], \tag{A.6}$$

$$\Delta_{\chi^0}\lambda_5 = -2i \int_k \left[g_2^2\mu M_2\Delta_1(k) + g_1^2\mu M_1\Delta_2(k)\right]^2 \Delta_\mu^2(k), \tag{A.7}$$

$$\Delta_{\chi^0}\lambda_6 = 2i \int_k k^2 \left[g_2^4 M_2\Delta_1^2(k) + g_2^2 g_1^2(M_2 + M_1)\Delta_1(k)\Delta_2(k) + g_1^4 M_1\Delta_2^2(k)\right]\mu\Delta_\mu^2(k)$$
$$= \Delta_{\chi^0}\lambda_7, \tag{A.8}$$

where

$$\Delta_1(k) = \frac{1}{k^2 - |M_2|^2}, \qquad \Delta_2(k) = \frac{1}{k^2 - |M_1|^2}, \qquad \Delta_\mu(k) = \frac{1}{k^2 - |\mu|^2}. \tag{A.9}$$

Note that M_2, M_1 and μ are complex.

In the special case of $M_2 = M_1$, the corrections to the effective parameters are reduced to

$$\Delta_{\chi^0}m_3^2 = 2\frac{g_2^2}{\cos^2\theta_W}\mu M_2 \cdot i \int_k \Delta_1(k)\Delta_\mu(k), \tag{A.10}$$

$$\Delta_{\chi^0}\lambda_5 = -2\frac{g_2^4}{\cos^4\theta_W}(\mu M_2)^2 \cdot i \int_k \Delta_1^2(k)\Delta_\mu^2(k), \tag{A.11}$$

$$\Delta_{\chi^0}\lambda_6 = \Delta_{\chi^0}\lambda_7 = 2\frac{g_2^4}{\cos^4\theta_W}\mu M_2 \cdot i \int_k k^2 \Delta_1^2(k)\Delta_\mu^2(k). \tag{A.12}$$

In this case, the contributions of charginos relate to those of neutralinos as

$$\Delta_{\chi^0}m_3^2 = \frac{1}{\cos^2\theta_W}\Delta_{\chi^\pm}m_3^2, \tag{A.13}$$

$$\Delta_{\chi^0}\lambda_5 = \frac{1}{\cos^4\theta_W}\Delta_{\chi^\pm}\lambda_5, \tag{A.14}$$

$$\Delta_{\chi^0}\lambda_6 = \Delta_{\chi^0}\lambda_7 = \frac{1}{\cos^4\theta_W}\Delta_{\chi^\pm}\lambda_6 = \frac{1}{\cos^4\theta_W}\Delta_{\chi^\pm}\lambda_7. \tag{A.15}$$

The mass-squared matrix of stops is given by

$$M_{\tilde{t}}^2 = \begin{pmatrix} m_{11}^2 & m_{12}^2 \\ m_{12}^{2*} & m_{22}^2 \end{pmatrix}, \tag{A.16}$$

where

$$m_{11}^2 = m_{\tilde{t}_L}^2 - \frac{1}{8}\left(\frac{g_1^2}{3} - g_2^2\right)(\rho_1^2 - \rho_2^2) + \frac{1}{2}y_t^2\rho_2^2, \tag{A.17}$$

$$m_{22}^2 = m_{\tilde{t}_R}^2 + \frac{1}{6}g_1^2(\rho_1^2 - \rho_2^2) + \frac{1}{2}y_t^2\rho_2^2, \tag{A.18}$$

$$m_{12}^2 = \frac{y_t}{\sqrt{2}}\left[(\mu\rho_1 + A_t\rho_2\cos\theta) - iA_t\rho_2\sin\theta\right]. \tag{A.19}$$

Here y_t is the top Yukawa coupling. $m_{\tilde{t}_L}^2$, $m_{\tilde{t}_R}^2$ and A_t are the soft-SUSY-breaking mass-squared parameters.

The formulas for the corrections to the effective parameters are

$$\Delta_{\tilde{t}}m_3^2 = -N_c y_t^2 \mu A_t^* \cdot i \int_k \Delta_1(k)\Delta_2(k), \tag{A.20}$$

$$\Delta_{\tilde{t}}\lambda_5 = N_c y_t^4 (\mu A_t^*)^2 \cdot i \int_k \Delta_1^2(k)\Delta_2^2(k), \tag{A.21}$$

$$\Delta_{\tilde{t}}\lambda_6 = -N_c y_t^2 \mu A_t^* \cdot i \int_k \left[\left(\frac{g_2^2}{4} - \frac{g_1^2}{12}\right)\Delta_1^2(k)\Delta_2(k) + \frac{g_1^2}{3}\Delta_1(k)\Delta_2^2(k)\right.$$
$$\left. + y_t^2|\mu|^2\Delta_1^2(k)\Delta_2^2(k)\right], \tag{A.22}$$

$$\Delta_{\tilde{t}}\lambda_7 = -N_c y_t^2 \mu A_t^* \cdot i \int_k \left\{\left[y_t^2 - \left(\frac{g_2^2}{4} - \frac{g_1^2}{12}\right)\right]\Delta_1^2(k)\Delta_2(k) + \left(y_t^2 - \frac{g_1^2}{3}\right)\Delta_1(k)\Delta_2^2(k)\right.$$
$$\left. + y_t^2|A_t|^2\Delta_1^2(k)\Delta_2^2(k)\right\}, \tag{A.23}$$

where

$$\Delta_1(k) = \frac{1}{k^2 - m_{\tilde{t}_L}^2}, \qquad \Delta_2(k) = \frac{1}{k^2 - m_{\tilde{t}_R}^2}. \tag{A.24}$$

In the case of $m_{\tilde{t}_R} \simeq 0$, the finite-temperature Feynman integrals become ill-defined because of infrared divergence. Then one should employ another method to evaluated the effective potential as done in [10]. B_2 and C_1 are extracted from the light stop contribution to the effective potential, which is treated by the high-temperature expansion (2.13).

References

[1] For a review see, A. Cohen, D. Kaplan and A. Nelson, Ann. Rev. Nucl. Part. Sci. **43** (1993) 27.
K. Funakubo, Prog. Theor. Phys. **96** (1996) 475.

[2] M. Carena, M. Quiros, C. E. M. Wagner, Phys. Lett. **B380** (1996) 81.

[3] D. Delepine, J.-M. Gerard, R. Gonzalez Felipe, J. Weyers, Phys. Lett. **B386** (1996) 183.

[4] M. Dugan, B. Grinstein and L. Hall, Nucl. Phys. **B255** (1985) 413.

[5] Y. Kizukuri and N. Oshimo, Phys. Rev. **D45** (1992) 1806; Phys. Rev. **D46** (1992) 3025.

[6] A. Nelson, D. Kaplan and A. Cohen, Nucl. Phys. **B373** (1992) 453.

[7] K. Funakubo, A. Kakuto, S. Otsuki, K. Takenaga and F. Toyoda, Prog. Theor. Phys. **94** (1995) 845.

[8] K. Funakubo, A. Kakuto, S. Otsuki and F. Toyoda, Prog. Theor. Phys. **98** (1997) 427.

[9] K. Funakubo, A. Kakuto, S. Otsuki and F. Toyoda, Prog. Theor. Phys. **96** (1997) 771.

[10] K. Funakubo, A. Kakuto, S. Otsuki and F. Toyoda, Prog. Theor. Phys. **99** (1998) 1045.

[11] M. Laine and K. Rummukainen, hep-ph/9811369.

[12] K. Funakubo, Prog. Theor. Phys. **101** (1999) in press.

[13] D. Comelli, M. Pietroni and A. Riotto, Nucl. Phys. **B412** (1994) 441.

[14] J. R. Espinosa, J. M. Moreno and M. Quiros, Phys. Lett. **B319** (1993) 505.

[15] J.M. Moreno, M. Quiros and M. Seco, Nucl. Phys. **B526** (1998) 489.
P. John, hep-ph/9810499.

[16] L. Dolan and R. Jackiw, Phys. Rev. **D9** (1974) 3320.

[17] A. Pilaftsis and C. E. M. Wagner, hep-ph/9902371.

[18] N. Maekawa, Phys. Lett. **B282** (1992) 387; Nucl. Phys. B (Proc. Suppl.) **37A** (1994), 191.

[19] J. R. Espinosa, Nucl. Phys. **B475** (1996) 273.
B. de Carlos and J. R. Espinosa, Nucl. Phys. **B503** (1997) 24

[20] K. Funakubo, A. Kakuto, S. Otsuki, K. Takenaga and F. Toyoda, Prog. Theor. Phys. **93** (1995) 1067.

[21] A. G. Cohen, D. B. Kaplan and A. E. Nelson, Phys. Lett. **B336** (1994) 41.

[22] The OPAL Collaboration, hep-ex/9811025.